Electronic Structures and Magnetic Order of Ordered-Fe-Vacancy Ternary Iron Selenides $TlFe_{1.5}Se_2$ and $AFe_{1.5}Se_2$ (A = K, Rb, or Cs)

Xun-Wang Yan,[1,2] Miao Gao,[1] Zhong-Yi Lu,[1,*] and Tao Xiang[2,3,†]

[1]*Department of Physics, Renmin University of China, Beijing 100872, China*
[2]*Institute of Theoretical Physics, Chinese Academy of Sciences, Beijing 100190, China*
[3]*Institute of Physics, Chinese Academy of Sciences, Beijing 100190, China*

(Received 20 January 2011; published 25 February 2011)

By the first-principles electronic structure calculations, we find that the ground state of the Fe-vacancies ordered $TlFe_{1.5}Se_2$ is a quasi-two-dimensional collinear antiferromagnetic semiconductor with an energy gap of 94 meV, in agreement with experimental measurements. This antiferromagnetic order is driven by the Se-bridged antiferromagnetic superexchange interactions between Fe moments. Similarly, we find that crystals $AFe_{1.5}Se_2$ ($A = \mathrm{K}$, Rb, or Cs) are also antiferromagnetic semiconductors but with a zero-gap semiconducting state or semimetallic state nearly degenerated with the ground states. Thus, rich physical properties and phase diagrams are expected.

DOI: 10.1103/PhysRevLett.106.087005 PACS numbers: 74.70.Xa, 74.20.Mn, 74.20.Pq

The discovery of high transition temperature superconductivity in LaFeAsO by partial substitution of O with F atoms [1] has stimulated great interest in iron pnictides. Other kinds of iron-based compounds were also reported to show superconductivity after doping or under high pressures [2–4]. A ubiquitous feature is that the parent compounds of these superconductors are antiferromagnetic (AFM) semimetals [5] with either a collinear [6,7] or bicollinear [8–10] AFM order below a structural transition temperature.

Very recently the superconductivity was discovered at about 30 K in the potassium intercalated FeSe-layer compound $K_{0.8}Fe_2Se_2$ [11]. Soon after, the superconductivity was also found in the Cs-intercalated compound $Cs_{0.8}(FeSe_{0.98})_2$ [12] and the (Tl, K)-intercalated compound $(Tl, K)Fe_xSe_2$ [13]. These compounds have the $ThCr_2Si_2$-type structure [Fig. 1(a)], isostructural with 122-type iron pnictides $BaFe_2As_2$ [2]. But they should be regarded as a new kind of iron-based superconductors since they are chalcogenides rather than pnictides. We have done the first-principles electronic structure calculations for these materials [14]. We find that their parent compounds $TlFe_2Se_2$ and AFe_2Se_2 ($A = \mathrm{K}$ or Cs) are also AFM semimetals and the ground states are in a bicollinear AFM order.

An important feature revealed by the latest transport measurement is that the superconductivity in Tl and K intercalated FeSe materials is proximity to an AFM insulating phase [13], similar to high-T_c cuprates. In particular, $TlFe_xSe_2$ ($1.3 < x < 1.7$) is found to be an AFM insulator, with an activated transport gap of $\sim$57 meV for $x = 1.5$ [13]. This has revived the discussion on the correlation effect in Fe-based superconductors.

To clarify this issue, we have performed the first-principles electronic structure calculations on $TlFe_{1.5}Se_2$ and $AFe_{1.5}Se_2$ ($A = \mathrm{K}$, Rb, or Cs). We find that the ground state of crystal $TlFe_{1.5}Se_2$ is indeed an AFM semiconductor with a collinear AFM order [Fig. 4(b)] and an energy gap of 94 meV, and similarly $AFe_{1.5}Se_2$ is also an AFM semiconductor but with a zero-gap semiconducting state or AFM semimetallic state close to the ground state. This is the first time theoretically to show there exists an AFM insulating state in Fe-based superconductor materials.

In our calculations the plane wave basis method was used [15]. We adopted the generalized gradient approximation (GGA) with Perdew-Burke-Ernzerhof formula [16] for the exchange-correlation potentials. The ultrasoft pseudopotentials [17] were used to model the electron-ion interactions. After the full convergency test, the kinetic energy cutoff and the charge density cutoff of the plane wave basis were chosen to be 800 and 6400 eV, respectively. The Gaussian broadening technique was used and a

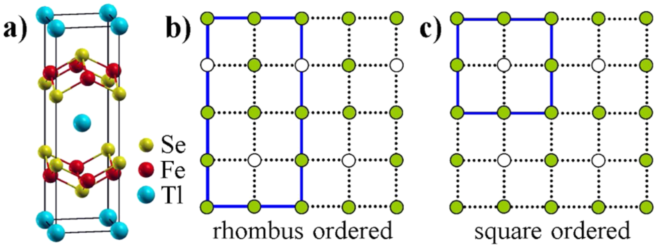

FIG. 1 (color online). $TlFe_xSe_2$ with the $ThCr_2Si_2$-type structure: (a) a tetragonal unit cell containing two formula units without any vacancy; (b) schematic top view of the Fe-Fe square layer with one-quarter Fe vacancies ordered in rhombus ($x = 1.5$), in which there are two inequivalent Fe atoms, namely, 2-Fe-neighbored and 3-Fe-neighbored Fe atoms. (c) Schematic top view of the Fe-Fe square layer with one-quarter Fe vacancies ordered in square ($x = 1.5$). The filled circles denote the Fe atoms while the empty circles denote the Fe vacancies. The square and rectangle enclosed by the solid lines denote the unit cells.

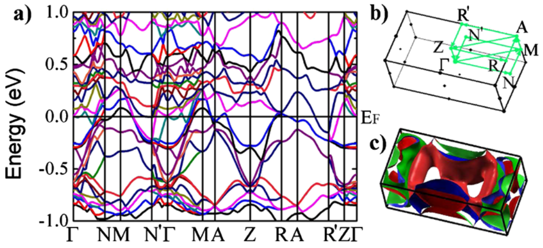

FIG. 2 (color online). Electronic structure of $TlFe_{1.5}Se_2$ with the Fe vacancies ordered in rhombus [Fig. 1(b)] in the nonmagnetic state: (a) the band structure, (b) the Brillouin zone, and (c) the Fermi surface. The Fermi energy sets to zero.

mesh of $18 \times 18 \times 9$ k points was sampled for the Brillouin-zone integration. In the calculations, the lattice parameters with the internal atomic coordinates were optimized by the energy minimization. For $TlFe_{1.5}Se_2$, the optimized tetragonal lattice parameters are found in excellent agreement with the experimental ones [13].

The early experiments suggested that the Fe vacancies in $TlFe_{1.5}Se_2$ are ordered in a rhombus structure, as shown in Fig. 1(b) [18]. In order to test theoretically whether this structure is truly the ground state, we have also calculated the electronic structure of another possible one-quarter Fe-vacancies ordered structure, namely, the square-ordered vacancy structure, as shown in Fig. 1(c). In the nonmagnetic state, we find that the energy of the square-ordered vacancy structure is lower by about 12 meV/Fe than the rhombus-ordered vacancy structure. It is noted that an Fe vacancy only induces small local structural deviation (less than 0.04 Å) from the original tetragonal one except for Tl atoms, which means the covalent bonding between Fe and Se atoms is rather robust. Figures 2 and 3 show the nonmagnetic band structures and Fermi surfaces of $TlFe_{1.5}Se_2$ in the Fe-vacancies rhombus- and square-ordered structures, respectively. In both cases, there are a number of electron and hole bands crossing the Fermi level. The Fermi surface nesting is not as strong as in the iron pnictides [5].

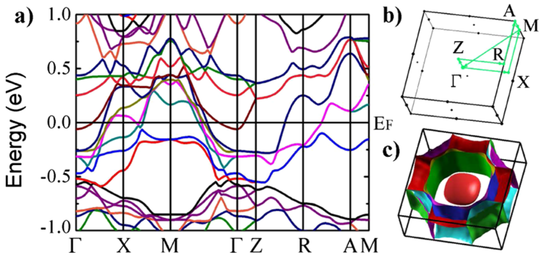

FIG. 3 (color online). Electronic structure of $TlFe_{1.5}Se_2$ with the Fe vacancies ordered in square [Fig. 1(c)] in the nonmagnetic sate: (a) the band structure, (b) the Brillouin zone, and (c) the Fermi surface. The Fermi energy sets to zero.

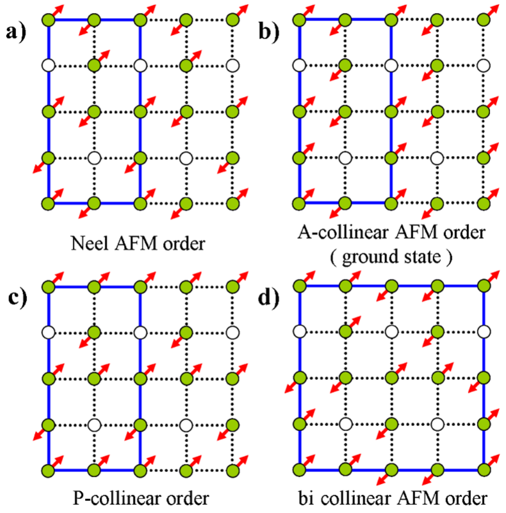

FIG. 4 (color online). Schematic top view of four possible magnetic orders in the Fe-Fe square layer with one-quarter Fe vacancies ordered in rhombus: (a) checkerboard Néel order in which the nearest-neighboring Fe moments are antiparallel ordered; (b) A-collinear AFM order in which the Fe moments are antiferromangtic ordered along the line without vacancies; (c) P-collinear AFM order in Fe moments are antiferromagnetic ordered along the lines with vacancies; (d) bicollinear AFM order. The squares or rectangles enclosed by the solid lines denote the magnetic unit cells.

However, in the true ground state which is in an AFM order, we find that the energy of the rhombus-ordered vacancy structure is lower by 15.1 meV/Fe than the square-ordered one. Figures 4 and 5 show a number of possible magnetic orders in the Fe-vacancies rhombus- and square-ordered structures, respectively. Among these magnetic ordered states, we find that the Fe-vacancies rhombus-ordered structure with an A-collinear AFM order shown in Fig. 4(b) has the lowest energy. This rhombus order of vacancies agrees with the neutron measurement [18]. Our result further suggests that the rhombus-ordered vacancy structure is stabilized by an A-collinear AFM order. In the A-collinear AFM state [Fig. 4(b)], the Fe moments are antiferromagnetically ordered along the lines without Fe vacancies and ferromagnetically ordered along the lines perpendicular.

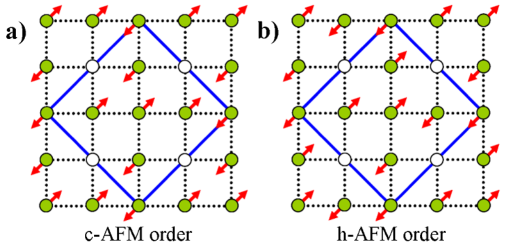

FIG. 5 (color online). Schematic top view of two possible magnetic orders in the Fe-Fe square layer: (a) c-AFM order in which the next-nearest Fe moments are antiparallel ordered; (b) h-AFM order in which half pairs of the next-nearest Fe moments are in antiparallel while the other half pairs are in parallel. The squares enclosed by the solid lines denote the magnetic unit cells.

Similar to the iron pnictides [19,20], we find that there is a small structural distortion in $\mathrm{TlFe_{1.5}Se_2}$. The lattice constant slightly expands along the AFM direction and contracts along the ferromagnetic direction in the *A*-collinear AFM state. This leads to a small energy gain of $\sim$1 meV/Fe. We also find that the Fe magnetic moments between the neighbor layers FeSe are antiferromagnetically ordered. The energy difference between the ferromagnetic and AFM interlayer magnetic states is $\sim$4.9 meV/Fe. Thus the ground state of $\mathrm{TlFe_{1.5}Se_2}$ is an *A*-collinear AFM state with AFM interlayers of FeSe.

Figure 6(a) shows the ground state electronic band structure of $\mathrm{TlFe_{1.5}Se_2}$. Unlike other parent compounds of iron pnictides or chalcogenides, $\mathrm{TlFe_{1.5}Se_2}$ is an AFM semiconductor, in agreement with experimental measurements. The energy band gap is found to be $\sim$94 meV, which is also consistent with the gap value obtained by the transport measurement, 57.7 meV [13]. The compound $\mathrm{TlFe_{1.5}Se_2}$ in the other magnetic orders is found to be mostly metallic.

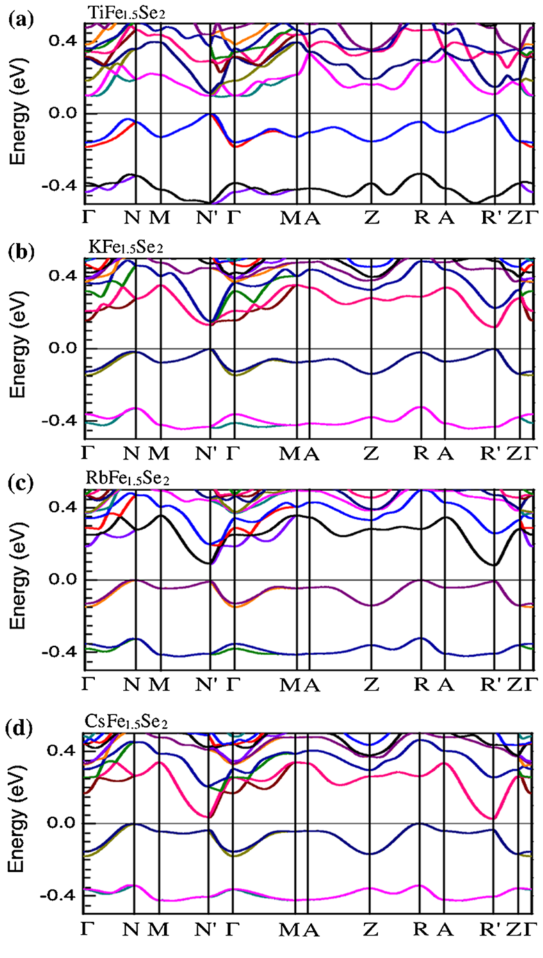

FIG. 6 (color online). Electronic band structure of $\mathrm{TlFe_{1.5}Se_2}$ or $A\mathrm{Fe_{1.5}Se_2}$ (A = K, Rb, or Cs) with one-quarter Fe vacancies ordered in rhombus [see Fig. 1(b)] and with an *A*-collinear AFM order [see Fig. 4(b)] in the ground state, which is an antiferromagnetic semiconductor. (a) $\mathrm{TlFe_{1.5}Se_2}$, (b) $\mathrm{KFe_{1.5}Se_2}$, (c) $\mathrm{RbFe_{1.5}Se_2}$, (d) $\mathrm{CsFe_{1.5}Se_2}$. The Brillouin zone is shown in Fig. 2(b). Here the top of the valence band sets to zero. Note that Γ-N(Γ-N') corresponds to the antiparallel- (parallel-)aligned moment line.

There are two inequivalent Fe atoms according to the number of neighboring Fe atoms if the Fe vacancies are rhombus ordered, namely, 2-Fe-neighbored and 3-Fe-neighbored Fe atoms, respectively [see Fig. 1(b)]. By projecting the density of states onto the five 3*d* orbitals of Fe (Fig. 7), we find that the five up-spin orbitals are almost completely filled on both kinds of Fe atoms. This suggests that the crystal field splitting induced by Se atoms is small, similar to iron pnictides. The magnetic moment formed around each Fe atom is found to be about $2.8\mu_B$. This large Fe magnetic moment apparently results from the Hund's rule coupling [19,20]. The down-spin orbitals are partially filled by d_{yz}, d_{xy}, and $d_{x^2-y^2}$ orbitals for the 2-Fe-neighbored Fe atoms or by d_{yz} and d_{xy} orbitals for the 3-Fe-neighbored Fe atoms. Such anisotropy among the five down-spin orbitals in $\mathrm{TlFe_{1.5}Se_2}$ results from the Fe vacancies.

Inspection of the real space charge distribution in $\mathrm{TlFe_{1.5}Se_2}$ shows that there is a strong covalence bond between the neighbor Fe and Se atoms. This gives rise to an effective AFM superexchange interaction bridged by the Se atoms between the next-nearest neighbor Fe moments, similar to iron pnictides [19,20]. If the energy of the nonmagnetic state is set to zero, we find that the energies of the ferromagnetic, checkerboard Néel AFM, *A*-collinear AFM, and bicollinear AFM states are ($-$ 0.114, -0.217, -0.326, -0.270) eV/Fe for $\mathrm{TlFe_{1.5}Se_2}$. The magnetic moment around each Fe atom is found to be about

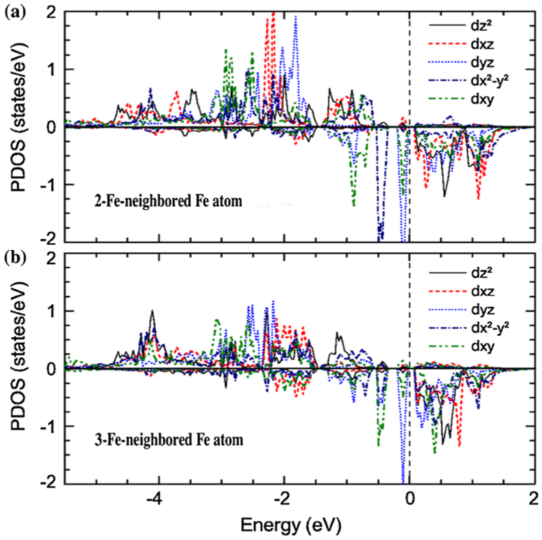

FIG. 7 (color online). Projected density of states (PDOS) at the five Fe-3*d* orbitals around (a) 2-Fe-neighbored Fe atom and (b) 3-Fe-neighbored atom in the *A*-collinear AFM ordered ground state of $\mathrm{TlFe_{1.5}Se_2}$. Here the top of the valence band sets to zero and *x* axis is along the antiferromagnetic direction while *y* axis is along the ferromagnetic direction in Fig. 4(b).

2.5–2.8μ_B, varying weakly in the above four magnetically ordered states, similar to the iron pnictides [19,20]. If we attribute the energy differences of these states entirely to the contribution of magnetic interactions between the spins $\vec{S}$ and model them by the simple Heisenberg model with the nearest (J_1), next-nearest (J_2), and next-next-nearest (J_3) neighbor interactions and ignore the anisotropy caused by the Fe vacancies [19], we find that $J_1 = 39\ \mathrm{meV}/S^2$, $J_2 = 60\ \mathrm{meV}/S^2$, and $J_3 = 7\ \mathrm{meV}/S^2$ for $\mathrm{TlFe_{1.5}Se_2}$. In obtaining these values, the contribution from itinerant electrons is ignored. Similarly, we find that $J_1 = 37\ \mathrm{meV}/S^2$, $J_2 = 64\ \mathrm{meV}/S^2$, and $J_3 = 8\ \mathrm{meV}/S^2$ for $\mathrm{KFe_{1.5}Se_2}$ (see below for more).

To quantify the electronic correlation effect in $\mathrm{TlFe_{1.5}Se_2}$, we have performed a GGA + U calculation. We find that the energy band gap increases dramatically with the Coulomb interaction U. When U is larger than 2 eV, the energy band gap is over 190 meV, which is significantly larger than the measurement value of 57 meV [13]. This suggests that the magnetic ordering and the energy band gap are driven mainly by the exchange effect, rather than the correlation effect.

Here we emphasize that the calculation convergency test needs to be elaborated. An enough high energy cutoff and a set of sufficient many k points are required to ensure the correct ground state, namely, an AFM semiconductor obtained. Otherwise, the calculations always yield a metallic state rather than semiconducting state.

We have further performed the first-principles electronic structure calculations for $A\mathrm{Fe_{1.5}Se_2}$ (A = K, Rb, or Cs). Like $\mathrm{TlFe_{1.5}Se_2}$, we find that crystal $A\mathrm{Fe_{1.5}Se_2}$ is an AFM semiconductor and its ground state is also an A-collinear AFM state with AFM interlayers of FeSe. Figures 6(b)–6(d) show the ground state electronic band structures for $\mathrm{KFe_{1.5}Se_2}$, $\mathrm{RbFe_{1.5}Se_2}$, and $\mathrm{CsFe_{1.5}Se_2}$, respectively. Accordingly, the energy band gaps are found to be 121, 69, and 26 meV for $\mathrm{KFe_{1.5}Se_2}$, $\mathrm{RbFe_{1.5}Se_2}$, and $\mathrm{CsFe_{1.5}Se_2}$, respectively.

The calculations show that the energies of $\mathrm{KFe_{1.5}Se_2}$, $\mathrm{RbFe_{1.5}Se_2}$, and $\mathrm{CsFe_{1.5}Se_2}$ in the A-collinear AFM order but with the ferromagnetic interlayers of FeSe are higher than the AFM interlayers of FeSe by 8.9, 5.2, and 2.8 meV/Fe, respectively. In such a case with the ferromagnetic interlayers of FeSe, crystals $\mathrm{TlFe_{1.5}Se_2}$ and $\mathrm{KFe_{1.5}Se_2}$ are both still AFM semiconductors with indirect band gaps of 20 and 32 meV and direct gaps of 46 and 62 meV, respectively. However, crystal $\mathrm{RbFe_{1.5}Se_2}$ becomes a zero-gap semiconductor while crystal $\mathrm{CsFe_{1.5}Se_2}$ becomes an AFM semimetal with the electron and hole carrier densities of $7.47 \times 10^{19}/\mathrm{cm}^3$ and $7.35 \times 10^{19}/\mathrm{cm}^3$, respectively. These two states, zero-gap semiconducting and AFM semimetallic, will significantly influence the physical properties of $\mathrm{RbFe_{1.5}Se_2}$ and $\mathrm{CsFe_{1.5}Se_2}$ since they are almost degenerated with the ground states.

Moreover, we also find that the square-ordered vacancy structure with a c-AFM order [Fig. 5(a)] and AFM interlayers of FeSe are metastable for crystal $A\mathrm{Fe_{1.5}Se_2}$ (A = K, Rb, or Cs). Energetically, it is just higher than the ground state by 10.9, 7.9, and 5.0 meV/Fe for $\mathrm{KFe_{1.5}Se_2}$, $\mathrm{RbFe_{1.5}Se_2}$, and $\mathrm{CsFe_{1.5}Se_2}$, respectively. Such a square-ordered vacancy structure pattern should thus have a certain probability of formation in the compound $A\mathrm{Fe_{1.5}Se_2}$.

In conclusion, we have performed the first-principles calculations for the electronic structure and magnetic order of $\mathrm{TlFe_{1.5}Se_2}$. We find that the crystal structure of $\mathrm{TlFe_{1.5}Se_2}$ with the rhombus-ordered Fe vacancies in a collinear antiferromagnetic order is energetically the most stable. The ground state of $\mathrm{TlFe_{1.5}Se_2}$ is a quasi-two-dimensional antiferromagnetic semiconductor with an energy gap of 94 meV. Our result is consistent with both neutron and transport measurements. We further predict that crystal $A\mathrm{Fe_{1.5}Se_2}$ (A = K, Rb, or Cs) is an antiferromagnetic semiconductor like $\mathrm{TlFe_{1.5}Se_2}$, and there is a zero-gap semiconducting state or antiferromagnetic semimetallic state nearly degenerated with the ground state for $\mathrm{RbFe_{1.5}Se_2}$ or $\mathrm{CsFe_{1.5}Se_2}$.

This work is partially supported by National Natural Science Foundation of China and by National Program for Basic Research of MOST, China.

---

*zlu@ruc.edu.cn
†txiang@iphy.ac.cn

[1] Y. Kamihara, T. Watanabe, M. Hirano, and H. Hosono, J. Am. Chem. Soc. **130**, 3296 (2008).
[2] M. Rotter, M. Tegel, and D. Johrendt, Phys. Rev. Lett. **101**, 107006 (2008).
[3] X. C. Wang *et al.*, Solid State Commun. **148**, 538 (2008).
[4] F.-C. Hsu *et al.*, Proc. Natl. Acad. Sci. U.S.A. **105**, 14 262 (2008).
[5] F. Ma and Z.-Y. Lu, Phys. Rev. B **78**, 033111 (2008).
[6] C. de la Cruz *et al.*, Nature (London) **453**, 899 (2008).
[7] J. Dong *et al.*, Europhys. Lett. **83**, 27 006 (2008).
[8] F. Ma *et al.*, Phys. Rev. Lett. **102**, 177003 (2009).
[9] W. Bao *et al.*, Phys. Rev. Lett. **102**, 247001 (2009).
[10] S. L. Li *et al.*, Phys. Rev. B **79**, 054503 (2009).
[11] Jiangang Guo *et al.*, Phys. Rev. B **82**, 180520(R) (2010).
[12] A. Krzton-Maziopa *et al.*, J. Phys. Condens. Matter **23**, 052203 (2011).
[13] M. Fang *et al.*, arXiv:1012.5236.
[14] X. W. Yan, M. Gao, Z. Y. Lu, and T. Xiang, arXiv:1012.5536.
[15] P. Giannozzi *et al.*, computer code QUANTUM ESPRESSO, http://www.quantum-espresso.org.
[16] J. P. Perdew, K. Burke, and M. Ernzerhof, Phys. Rev. Lett. **77**, 3865 (1996).
[17] D. Vanderbilt, Phys. Rev. B **41**, 7892 (1990).
[18] H. Sabrowsky *et al.*, J. Magn. Magn. Mater. **54–57**, 1497 (1986).
[19] F. Ma, Z. Y. Lu, and T. Xiang, Phys. Rev. B **78**, 224517 (2008).
[20] F. Ma, Z. Y. Lu, and T. Xiang, Front. Phys. China **5**, 150 (2009).